Biosynthesis of Silver/Iron Layered Double Hydroxide Alginate Beads for Amoxicillin Removal from Water

Dalal Ghanim Yahia[1,2]*, Ayad A. H. Faisal[1]

[1] Department of Environmental Engineering, College of Engineering, University of Baghdad, Baghdad 10011, Iraq
[2] Ministry of Transportation, Department of Designs and Engineering Consultancy, State Company for Implementation of Transport Projects, Baghdad 10011, Iraq

Corresponding Author Email: dalal.yahia2011d@coeng.uobaghdad.edu.iq

ABSTRACT

Ecosystems are being seriously threatened by the discharge of chemicals of new concern, such as antibiotics, into the environment. These pollutants were reported to be eliminated via adsorption, even at low concentrations and in a range of pH levels. Antibiotics have recently been removed using biomass-based adsorbent materials because of their affordability, high surface qualities, eco-friendliness, and widespread availability. Thus, the aim of this work is to produce a new sorbent using extracts from pomegranate peels and sesban tree leaves as precursors. Solutions extracted from pomegranate peels and sesban tree leaves can be used effectively to prepare silver and iron ions respectively. Silver-iron nanoparticles can be immobilized in the form of sodium alginate spherical beads. The prepared sorbent, named silver/iron-layered double hydroxide-sodium alginate beads (Ag/Fe-LDH-Na alginate beads), was tested for its ability to remove amoxicillin (AMO) from the aquatic environment in a batch study. The optimal conditions for preparing the aforementioned beads were an Ag/Fe molar ratio of 0.5, an initial pH of 9, and a mass of Ag/Fe-LDH nanoparticles of 7 grams per 100 mL. To remove more than 90% AMO, the best operational conditions were 90 minutes, initial pH 7, beads mass 2 grams per 50 mL, and speed 250 rpm for initial concentration (C_o) of 50 mg/L. The Langmuir model adequately describes sorption process suggesting a maximal capacity of 9.512 mg/g. Pseudo first-order and second-order models also provide a good description of the sorption process. The beads' characterization tests revealed the formation of Ag/Fe-LDH nanoparticles, which can be considered the main constituents of the new sorbent responsible for removing AMO, with the presence of functional groups such as the carboxylate (-COO) group. Antibiotic sorption is indicated by greater C percentage. The outcomes demonstrated that the prepared beads are highly reusable and reliable, thus making them effective in removing AMO from water, particularly in real-world applications.

1. INTRODUCTION

Environmental contamination with drugs and antibiotics has risen in recent years as a result of population growth and industrial expansion. It is growing into one of the most significant environmental issues. Consumption of antibiotics results in their entry into the food chain because they are used to treat diseases and improve health in human societies. As a result, these chemicals have the potential to persist in the environment over extended periods of time and emerge as pollutants. An over-the-top utilization of medications and anti-microbials can make opposition in microscopic organisms, which can prompt issues like the development of medication safe sicknesses [1].

Eliminating antibiotics from water and wastewater is a complex task that needs practical and scientific approaches. The approaches may be represented by applying active nanoparticles (NPs), nano-filtration, biological activities, physical and filtration methods, adsorption, as well as oxidation-ultrasonic methods. The use of nano-sorbents for removing of antibiotics from contaminated water considers efficient and new approach for controlling water pollution due to their efficiency and selectivity. Because of physicochemical characteristics of nano-sorbents, like light absorption, thermal and electrical conductivity, catalytic activity, wettability, melting point, quantum confinement, and dispersed without agglomeration, nano-sorbents have acquired prominence in technological development [2-4].

Antimicrobial resistance has become more likely as a result of antibiotic contamination. Amoxicillin is frequently used to treat animal and human bacterial infections. Environmental matrices often include amoxicillin and its metabolite. Amoxicillin also causes ecotoxicity to organisms that are not its intended targets.

It is commonly stated that antibiotics are present in the environment, particularly in sediments, surface water, and

groundwater. Water bodies are now contaminated with antibiotics as a result of rapid industrial growth and urbanization. The primary cause of antibiotic pollution is the excretion of unmetabolized antibiotics by living organisms. Additional causes include the pharmaceutical industry's dumping of leftover medications and hospital wastewater discharge, which raises the environmental burden of resistant microorganisms.

Due to its extreme instability, amoxicillin is easily hydrolyzed and rapidly breaks down into a variety of degradation products. Many biotic and abiotic mechanisms have the ability to cleave the beta-lactam ring. The most commonly recommended drugs in European nations are amoxicillin by itself or in conjunction with clavulanic acid. It is an antibiotic that is semi-synthetic and developed from amino-penicillin [1].

Many nano-sorbents have been researched and studied for the elimination of antibiotics from wastewater, including silica, carbon, zinc oxide NPs, and metal NPs such as gold, silver, and iron [2]. Recently, using metal–organic frameworks (MOFs) as nano-sorbents in the sorption process has gained great attention. Due to their structural complexity, MOF materials are highly effective in enhancing the elimination of various types of drug residues from wastewater. By varying the type of metal or organic compound used in the production of these materials, the sorption properties can be tailored for the capture of various types of drugs [3].

Methotrexate was adsorbed from water by Cr-MIL-101 NPs, and the results demonstrated that this nano-sorbent selectively sorbed Methotrexate with the highest efficiency [4]. Because it is easy to recover, this sorbent can be used again. Analgesics like paracetamol are used to treat fever and pain. It is commonly found in the municipal wastewater. The UIO-66 NPs were utilized for the sorption of Paracetamol from water. Such NPs have proved to have a high capability for capturing Paracetamol in polluted water. Additionally, the combination of two MOFs results in a new configuration with a higher surface area; therefore, it is possible to sorb larger drug molecules [5]. UIO-66 NPs, synthesized by the hydrothermal method, are considered nano-hybrids based on MOFs that can be used as an effective nano-sorbent for the adsorption of amoxicillin. This sorbent was synthesized from 1,4-benzene dicarboxylic acid and Zirconium metal.

Manufacturing of metallic nanoparticles (MNPs) is gained a lot of attention because of their physicochemical characteristics, high mono-dispersity and small size [6, 7]. MNPs, especially those made of silver, copper, and zinc, have gained a lot of attention and established themselves as a new sort of NPs [8]. Due to their usage in biosensor materials, composite fibers, wastewater treatment, pollution remediation, cosmetics, food packaging, and water purifiers, silver nanoparticles (Ag NPs) have received particular interest [9-13]. NPs are manufactured by different methods like chemical, physical, and biological techniques. Traditional ones (physic-chemical techniques) are applied for the preparation of Ag NPs. However, they have disadvantages such as the utilization of hazardous reactants, unstable yields, complicated purifications, environmental risks, less effective conversion, high consumption of energy, and expensive [14].

NPs prepared by biological method are far superior in comparison to those prepared by conventional ones. Algae, plants, and microorganisms can all utilize in the biological approach. The biological approach does, however, have drawbacks because it requires more time and involves challenging steps to maintain on the microbial cultures. The NPs can be prepared from flowers, roots, stems, and leaves due to their rapid formation, natural availability, inexpensive, efficient, and the ecofriendly nature [15-17]. Plants contain phytochemicals like flavonoids, saponins, alkaloids, terpenoids, phenolics, amino acids, proteins, polysaccharides, and vitamins which represent as capping, stabilizing and reducing agents for NPs bio-synthesis [18, 19].

Moreover, the sesban plant was chosen to contribute to reducing the waste of these trees, as they are cut at the beginning of winter every year in Iraq to eliminate or reduce the negative effects on the environment resulting from burning or throwing away this waste. Thus, the sesban leaves were chosen as a material used in this research paper to extract iron ions.

The extraction of silver and iron ions from pomegranate peels and sesban tree leaves respectively to reduce the influence of such solid wastes on the environment is the principal idea of this work. The extracted elements are mixed to obtain nanoparticles which immobilized using sodium alginate to produce silver-iron-LDH beads. The effectiveness of the prepared beads in reclaiming water containing the amoxicillin (AMO) antibiotic can be specified by: 1) finding the suitable parameters for AMO-beads interaction based on the batch tests with aid of familiar equilibrium and kinetic models, and 2) characterizing this interaction by tracking the variation in the active functional groups and morphology-elemental composition.

2. EXPERIMENTAL WORK

2.1 Materials

Amoxicillin (AMO) is the target contaminant that investigated in this study. It was provided by the Iraqi Samarra Pharmaceutical Company.

A one-liter aqueous solution containing 1000 mg of AMO was created for experimentation. The stock solution at room temperature required adjustment of its acidity by 0.1 M HCl and NaOH in incremental amounts. This solution must be diluted during batch studies in order to get the desired concentration of AMO. The antibiotic concentration is quantified by UV-visible spectrophotometer (England; Varian Cary 100 conc.) at a wavelength of 230 nm [20, 21].

Table 1. Characteristics of amoxicillin compound used as target contaminant in the current investigation
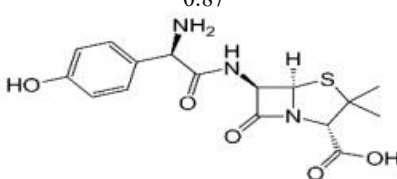
Property	Value or Description
Formula	$C_{16}H_{19}N_3O_5S$
Molecular weight (g/mol)	365.404
Solubility (mg/L)	3430
log K_{ow}	0.87
Chemical structure	

Table 1 shows the AMO feature used to show the effectiveness of prepared beads in the reclamation of water contained AMO antibiotic.

2.2 Extraction of silver

Silver ions was extracted from Pomegranate peels. Firstly, the peels were separated from other parts like seeds, membranes and fruit; rinsed with distilled water (DW) and must dry for 5 days in the air to remove the moisture and then grinding to small pieces. The 5 grams of such pieces were incorporated with 100 mL DW and the mix must be heated to 60°C for 15 minutes. This mixture must be passed through filter paper "0.45 μm pore size" and used as fresh extract in the next step. The 2.2 g of silver nitrate was dissolved (with absence of light) in 250 mL DW and heated to 60°C under stirring. Finally, 50 mL of pomegranate peel extract was collected with 100 mL deionized water and added drop wise using burette under stirring. The 50 mL of diluted pomegranate peel was added and then the mixture was left under stirring. The conversion of Ag+ to AgO was checked by addition one drop of 0.1 M HCl to the formation of white precipitate indicates that Ag+ was still in the solution. Therefore, the addition of pomegranate peels was completed until no white precipitate formed. Figure 1(a) describes the extraction of silver ions from pomegranate peels.
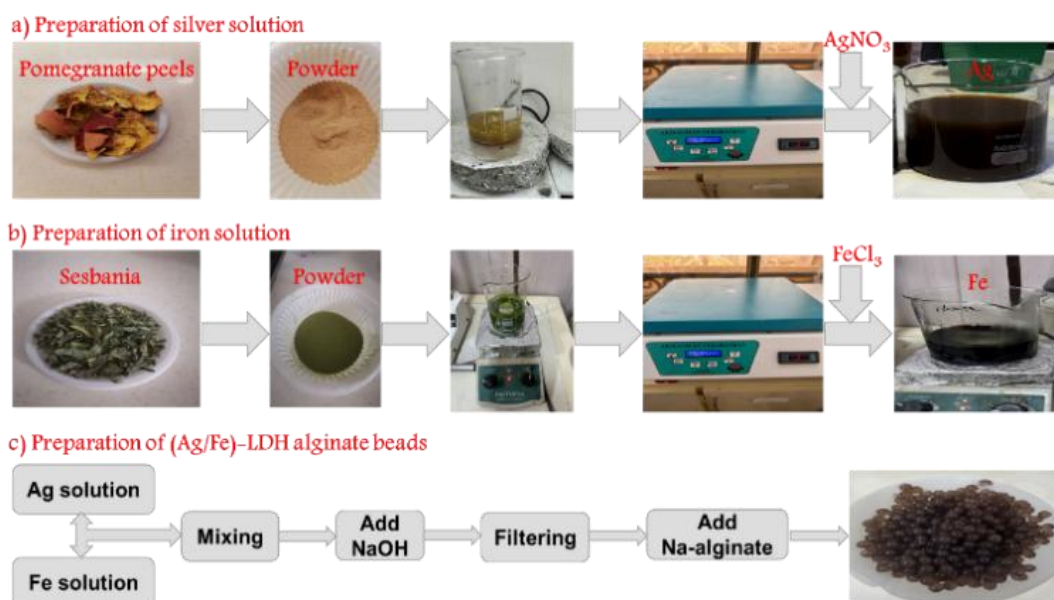

Figure 1. Block diagram for experimental procedure applied in the synthesis of (Ag/Fe)-LDH alginate beads

2.3 Extraction of iron

To extract the iron ions, the fresh sesbania leaves have rinsed with tap water, and then with DW. In addition, fresh Seban leaves were collected from Al-Krayat nurseries in Baghdad to produce iron nanoparticles. Pre-treatment was performed including washing and drying for sesbania leaves. At the beginning, the leaves rinsed with tap water and then with DW. After that, the leaves are dried for 5 days to remove the moisture and grinded into fine powder.

Thereafter, 5 grams of sesbania powder must mix with 100 mL DW. The mixture was heated to 60°C for 15 min and then passed through filter paper "0.45 μm pore size". The 2.16 g of ferric chloride ($FeCl_3$) must dissolve in 83.3 mL DW and heated to 40°C under stirring. After that, 50 mL of sesbania extract must dilute to 100 mL using DW and was added drop wise using burette under stirring and heated to 40°C. Figure 1(b) explains the extraction of iron from pomegranate peels.

2.4 The synthesis of Ag/Fe composite

The manufacturing Ag/Fe is required to add 100 mL of silver solution to the 100 mL of iron solution and the mixture must be agitated for 3 hours on the magnetic stirrer at 250 revolutions per minute. Then, the resultant substance can separate from aqueous solution by filtration; however, this substance must be dried at 60°C throughout the night. The main concept employed in the production of alginate beads; consisted of silver and iron, involves the immobilization of Ag/Fe nanoparticles in the polymer matrix of Na-alginate (a food-grade substance/ China) with 2.5×10^5 g/mol molecular weight. The manufacture procedure for Ag/Fe-LDH- alginate beads can be illustrated in Figure 1(c). The pH of this combination can adjust by 1 M NaOH solution which will be prepared with several concentrations, specifically around 7, 9 and 11. Moreover, the addition of NaOH (1 M) raises the pH to a desired level. The addition of alginate beads causes a significant shift in pH. As a result, the pH needs to be adjusted again to a neutral or slightly basic level. A variety of values were tested such as 7, 9 and 11.

The pH must increase to facilitate the creation of silver-iron nanoparticles, which were stirred for three hours at 250 revolutions per minute.

Sodium alginate was synthesized using the identical methodology described in earlier scientific publications. This methodology includes the dissolution 2 grams of Na-alginate per one hundred milliliters of DW. The solution should be properly mixed using stirrer for 24 h at room temperature. Different amounts of preformed nanoparticles have been introduced into a sodium alginate solution. The slurry must mix with 0.1 M $CaCl_2$ solution, which may prepare by dissolving 1-gram $CaCl_2$ in 100 mL DW. This is done to initiate polymerization and create beads by utilizing syringe of 10 mL. The beads, with 4 mm diameter, must be dried at 105°C. The beads have immersed in this solution for one hour; then, rinsed with DW and stored in 5 mM solution of $CaCl_2$ (0.278-gram $CaCl_2$ dissolved in 500 mL DW) at a temperature of 4 degrees Celsius for future use [22]. The AMO elimination efficiency was used as the indicator to determine the suitable conditions for preparation of beads, including Ag/Fe ratio,

dose of Ag/Fe nanoparticles, and solution's pH.

In addition, UV-visible spectroscopy was then used to examine the impact of the relative ratios of Ag/Fe synthesis. Preliminary tests revealed that the plant extract and Ag/Fe increased the UV-vis spectrum when combined in a 1:1 (v/v) ratio. The removal efficiency was regarded as high at this ratio. Generally speaking, absorbance maximum intensities rose as plant extract levels rose from 10% to 50%, while absorbance maximums fell as plant extract levels dropped from 60% to 10%. When both reactants were utilized in a 1:1 (v/v) ratio, the maximum absorbance with a somewhat narrow peak was observed. Nevertheless, the distinctive peak for silver nanoparticles was absent from the other (v/v) ratio of synthesis Ag/Fe.

2.5 Batch methodology

The adsorption of AMO onto prepared beads was investigated by batch tests conducted at temperature of room. To determine the best values of operational parameters (such as initial pH, agitation time, quantity of beads (m), and shaking speed), a series of tests were conducted for a specific C_o of AMO. The goal was to remove the highest quantities of the target pollutant. Insert 100 mL of simulated polluted water (V) into a flask with a specific C_o. Repeat this process in many flasks, each with a capacity of 250 mL. Various amounts of beads have combined with water in the flasks and agitated for 3 hours at 250 rpm. Subsequently, filter paper was employed to separate between beads and water, allowing for the measurement of the equilibrium concentration (C_e) of AMO using a UV-visible spectrophotometer. Eq. (1) [13] applies to find the AMO sorbed onto beads at equilibrium (q_e). The operational conditions adopted in the present study were contact time of 180 minutes, pH in the range from 3 to 11, the C_o ranging from 50 to 250 mg/L, and beads mass of 0.25-2 g per 50 mL.

$$q_e = (C_o - C_e) * \frac{V}{m} \qquad (1)$$

The AMO removal efficiency (R) onto prepared beads can calculate by the following equation:

$$R = \frac{(C_o - C_e)}{C_o} * 100 \qquad (2)$$

The recyclability of the exhausted material utilized in the study was evaluated. The regenerated process involved using a 0.1M sodium hydroxide solution to remove AMO. The efficacy of regenerated operation in eliminating AMO from contaminated water was investigated in a subsequent series of tests using the same optimal operational settings as indicated earlier, with a total of 6 regeneration cycles.

3. MODELING OF SORPTION MEASUREMENTS

The equilibrium isotherm models are employed to mathematically formulation of adsorption process. The models illustrate the correlation between the adsorbed and dissolved concentration of AMO. An increase in the concentration can lead to an increase in the removed amount of AMO; however, this relationship is not straightforward [23]. An isotherm is considered "favorable" when there is a

high concentration of contaminant onto the sorbent and a low concentration in the solution.

The equilibrium models are categorized into two kinds: the 1st type, including models such as Freundlich, Langmuir, Sips, Temkin, and Toth, applies to single component systems. The 2nd type, including models like the extended Langmuir model, extended Freundlich model, and Langmuir-Freundlich model, describes multicomponent systems. The models utilized in this work are the Freundlich model (Eq. (3)) and the Langmuir model (Eq. (4)). The Eq. (3) is suitable for describing the sorption of many layers onto nonhomogeneous surfaces, while the Langmuir model is applicable for describing the interaction of a single layer.

$$q_e = K_F * C_e^{\frac{1}{n}} \qquad (3)$$

$$q_e = \frac{q_{max} * b \, C_e}{1 + bC_e} \qquad (4)$$

where, K_F is the constant of Freundlich and q_{max} represents the highest capacity of sorption.

The temporal interaction between the sorbent and contaminant yielded a distinct set of outcomes in the context of kinetic sorption studies. The measurements are formulated by Eq. (5) (pseudo-first-order) and Eq. (6) (pseudo-second-order) models. The primary outcome of kinetic models is the determination of sorption rate by finding K_1 and K_2 [24].

$$q_t = q_e * (1 - e^{-K_1 * t}) \qquad (5)$$

$$q_t = \frac{K_2 * q_e^2 * t}{(1 + K_2 * q_e * t)} \qquad (6)$$

Kinetic measurements also must analyze by diffusion model (Eq. (7)) in order to accurately determine the key mechanisms that govern the AMO sorption.

$$q_t = k_{int} t^{0.5} + C \qquad (7)$$

where, k_{int} is the sorption rate constant (mg/g min$^{0.5}$), and C is the intercept that explained the thickness of boundary layer.

4. RESULTS AND DISCUSSION

4.1 Manufacturing of alginate beads

The investigation focused on determining the manufacturing conditions of prepared beads for adsorbing AMO from water. The operational conditions include initial pH of water, molar ratio of silver to iron, and quantity of silver - iron nanoparticles. The best value of each condition is identical to the higher AMO removal.

The impact of pH on the effectiveness of the manufactured sorbent was tested by altering pH from 7 to 11, with a molar ratio of 1 for Ag/Fe and (Ag/Fe)-LDH nanoparticles dosage of 5 g/100 mL. Experiments were performed to investigate the sorption properties using 1 grams of alginate per 50 milliliters of solution, with a concentration of 100 milligrams per liter of AMO solution, pH 7, and speed 250 revolutions per minute for 3 hours. Figure 2(a) illustrates the impact of pH on the effectiveness of sodium alginate in removing AMO during the production process. The highest efficiency of removed AMO

is observed at pH 9, with a value of 35.04%. Deviations from this pH level could lead to a significant decrease in efficiency, due to increase in the diameter of nanoparticle. Therefore, the manufacturing can achieve at pH 9.
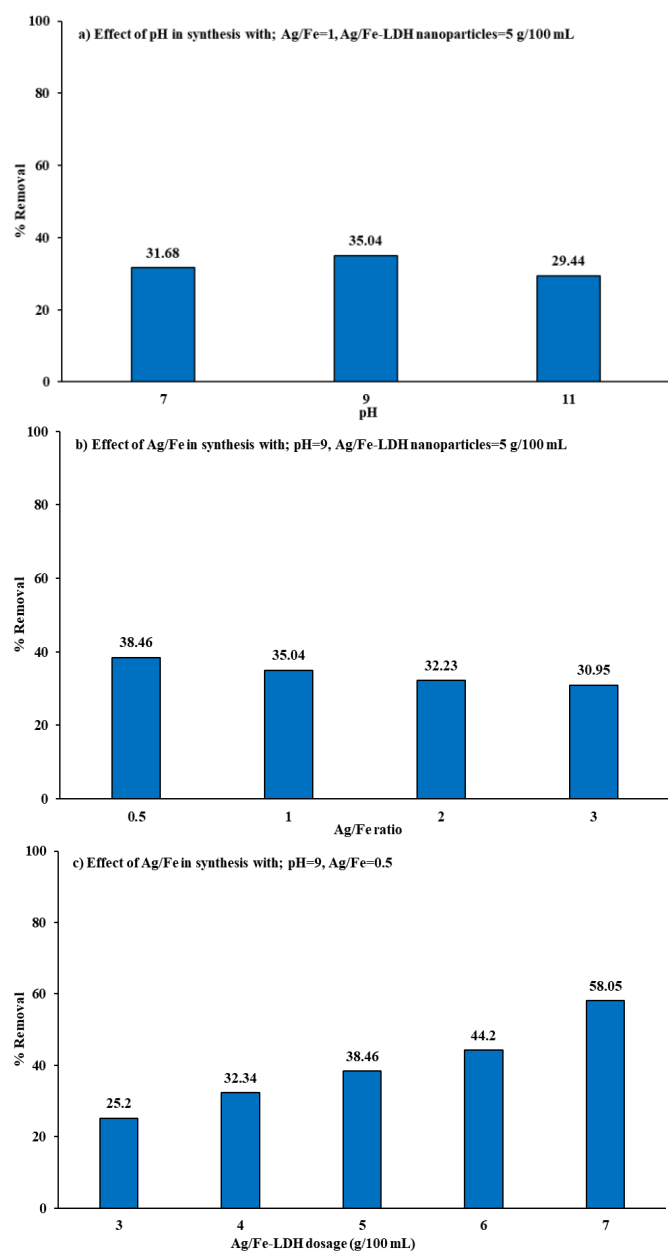

Figure 2. Effect of a) pH, b) Ag/Fe ration and c) Ag/Fe-LDH dosage on the AMO removal efficiency by prepared beads for sorption conditions (time=3 h, C_o=100 mg/L, sorbent dosage=1 g/50 mL, pH 7, speed 250 rpm)

The impact of silver to iron ratio, ranging from 0.5 to 3, on the production of beads can assess in an experiment conducted at pH 9. The applied dose of (Ag/Fe)-LDH nanoparticles was 5 grams per 100 mL. The results of Figure 2(b) demonstrate that the higher efficiency (38.46%) was achieved at a molar ratio of 0.5. The decrease in efficiency, as compared to the highest level, may be attributed to the structural disorder of the adsorbent's LDHs or the change in radius difference between Fe and Ag [25].

The impact of nanoparticles mass on the manufacture of beads can examine in the range from 1 to 7 grams per 100 mL for pH 9 and molar ratio of 0.5; However, results have been plotted in Figure 2(c). The outputs explain the presence a

significant improvement in the efficiencies of AMO removal. When the amount of alginate beads is increased from 1 to 7 gram, the efficiency of AMO removal can reach to 58.05%.

Based on the results above, the pH 9, Ag/Fe molar ratio 0.5, and nanoparticle dose 7 g/100 mL were optimal. To relate these findings to nanoparticle stability or surface chemistry, techniques are described that offer quantitative metrics for assessing and simulating the stability of nanoparticles with respect to their size, shape, surface chemistry, and core composition. Aggregation state also affects solution-phase nanoparticle stability. Nonetheless, the connection between the stability of nanoparticles and the physical/chemical characteristics Ag/Fe nanoparticles is examined. Particular definitions are examined in relation to surface chemistry, size, shape, core composition, and aggregation state. These same nanoparticle features are then linked to the definition of processes that promote nanoparticle stability. Once the optimum conditions were appeared in the solution, stable suspensions could be performed.

4.2 Conditions in batch tests

Figure 3 illustrates the influence of different factors on the efficacy of prepared beads in removing AMO from polluted water. These factors include: a) contact time, b) C_o, c) initial pH, d) speed of shaking, and e) beads mass. The operational settings include; time ≤ 180 minutes, C_o 100 mg/L, pH 7, sorbent mass 0.5 g per 50 mL of contaminated water, and speed 250 rpm. The AMO is rapidly eliminated during the initial stage of time and this elimination rate decreases beyond 90 minutes due to a reduction in the vacant sites available for AMO [26]. Figure 3(a) demonstrates that the approximately 58% of C_o 100 mg/L can be removed within 90 minutes. However, there is no significant change in removal percentages observed until 180 minutes.

Figure 3(b) shows the presence of clear reduction in the antibiotic capture efficiencies onto prepared beads as function of C_o. The removal efficiency decreased from 66.84% for 50 mg/L to 29.3% for 250 mg/L. The experiments were conducted for 90 minutes, pH 7, beads mass 1 g per 50 mL at 250 rpm. It is expected that all AMO molecules have the ability to interact with vacant sites of sorbent at low C_o. This interaction is likely to significantly enhance the sorption efficiency. However, when the AMO concentration rises while the mass of the sorbent remains constant, there is a possibility that the efficiency of sorption may decrease [27].

The pH of contaminated water is a crucial factor in the removal of antibiotics when water comes into contact with prepared beads. The pH may effect on the surface charge of sorbent, the ionization degree, and the functional groups dissociation [28]. Figure 3(c) illustrates the AMO removals as a function of pH values ranging from 3 to 11. The efficiency was low (≈ 45%) at pH 3 due to the competition between the AMO and hydrogen ions, which is likely the primary factor influencing this outcome. As the pH approaches neutrality, there is a noticeable improvement in the sorption efficiency, with values exceeding 60% for pH 7. The ionization and hydration of AMO may reduce in neutral conditions, hence the removal can be enhanced through p-p stacking effects and hydrogen bonding. The data presented in this figure indicates a drop in removal efficiency at greater pH because of the formation of hydroxide ions, which lead to reduce in hydrogen bonding. When pH < pH_{pzc}, the surface of sorbent carries a positive charge; conversely, the negative charge can be formed.

As pH < 7, there was a notable reduction in the zeta potential values. Consequently, the ability of AMO to be adsorbed onto the beads at such level was limited because of the electrostatic attraction.
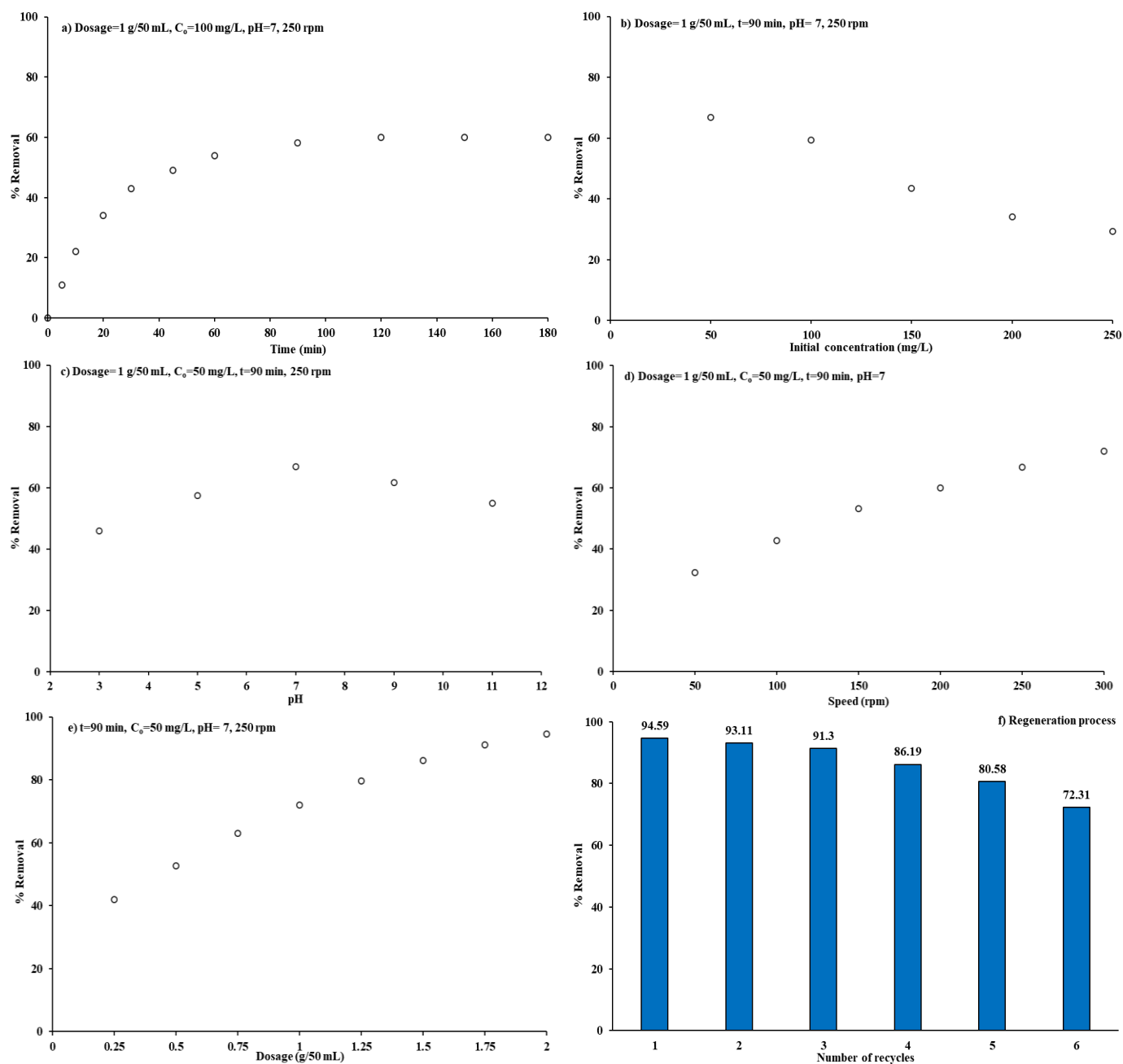

Figure 3. Effect of batch conditions on AMO removal from aqueous solution by prepared beads at room temperature (a-e), as well as (f) the regeneration process for exhausted beads

Figure 3(d) demonstrates that a high agitation speed significantly enhances the removal of AMO from polluted water. The removal efficiencies of AMO in stagnant aqueous solutions did not surpass 33%. However, these efficiencies significantly rose to 66.83% when the conditions were set to 200 rpm for 90 minutes, pH 7, beads mass of 1 gram per 50 mL, and C_o 100 mg/L. Figure 3(d) signifies that the higher speed (> 250 rpm) can lead to insignificant alteration in the sorption efficiency. In order to achieve a higher shaking speed, it is necessary to ensure that the antibiotic molecules come into proper contact with the alginate beads. This will enhance the movement of AMO molecules to the sorbent and ultimately improve the effectiveness of their removal.

Figure 3(e) represents the impact of sorbent amount on the AMO removal. Variation of dose with (0.25- 2 g) clearly improve the removal efficiencies for the antibiotic, with lowest value of 41.99% increasing to no less than 90%. It is clear that an increase in the amount of beads can improve the removals of AMO molecules [29].

4.3 Recyclability

To find the possibility of using exhausted (Ag/Fe)-LDH beads for the removal of AMO, a series of experimental studies were carried out, as shown in Figure 3(f). The outcome of these tests relies on the execution of adsorption-desorption cycles. The regeneration depends on the desorption of contaminants from the exhausted beads by the use of 0.5 M HCl solution. Figure 3(f) illustrates the relationship between

the removals of AMO and the number of recycling times. This relationship serves as an indicator of the regeneration effectiveness of (Ag/Fe)-LDH beads. It is evident that efficiency was diminished as the number of recycling processes increased, and more than 80% can be eliminated after 6 cycles. The results showed that the manufactured sorbent is highly reusable and reliable, making it an effective solution for removing AMO contaminants from water, particularly in real-world applications.

Leaching is a fascinating phenomenon that occurs when nanoparticles interact with liquids. It might be suggested that the leaching could be the responsible for the eliminating the removal efficiency as the number of recycling process increased. The removal efficiency reached 80% after six cycles.

4.4 Characterization of beads

The materials' crystalline structure, used in the manufacturing of present beads, was determined by "X-ray diffraction (XRD) analysis". Figure 4(a) plots the XRD for Ag, Fe, and Ag/Fe-LDH beads. Several diffraction reflections (Figure 4(a)) can be identified at specific intensities, represented by 2θ (degree) values at 13.5, 20.4, 32.2, 43.6, and 45.1. The reflections are corresponded to the active sites responsible for the AMO removal from water. According to the "Joint Committee on Powder Diffraction Standards (JCPDSs)", the reflections match exactly the Ag/Fe-LDH nanoparticles and this can certify the successful of production process [30, 31].
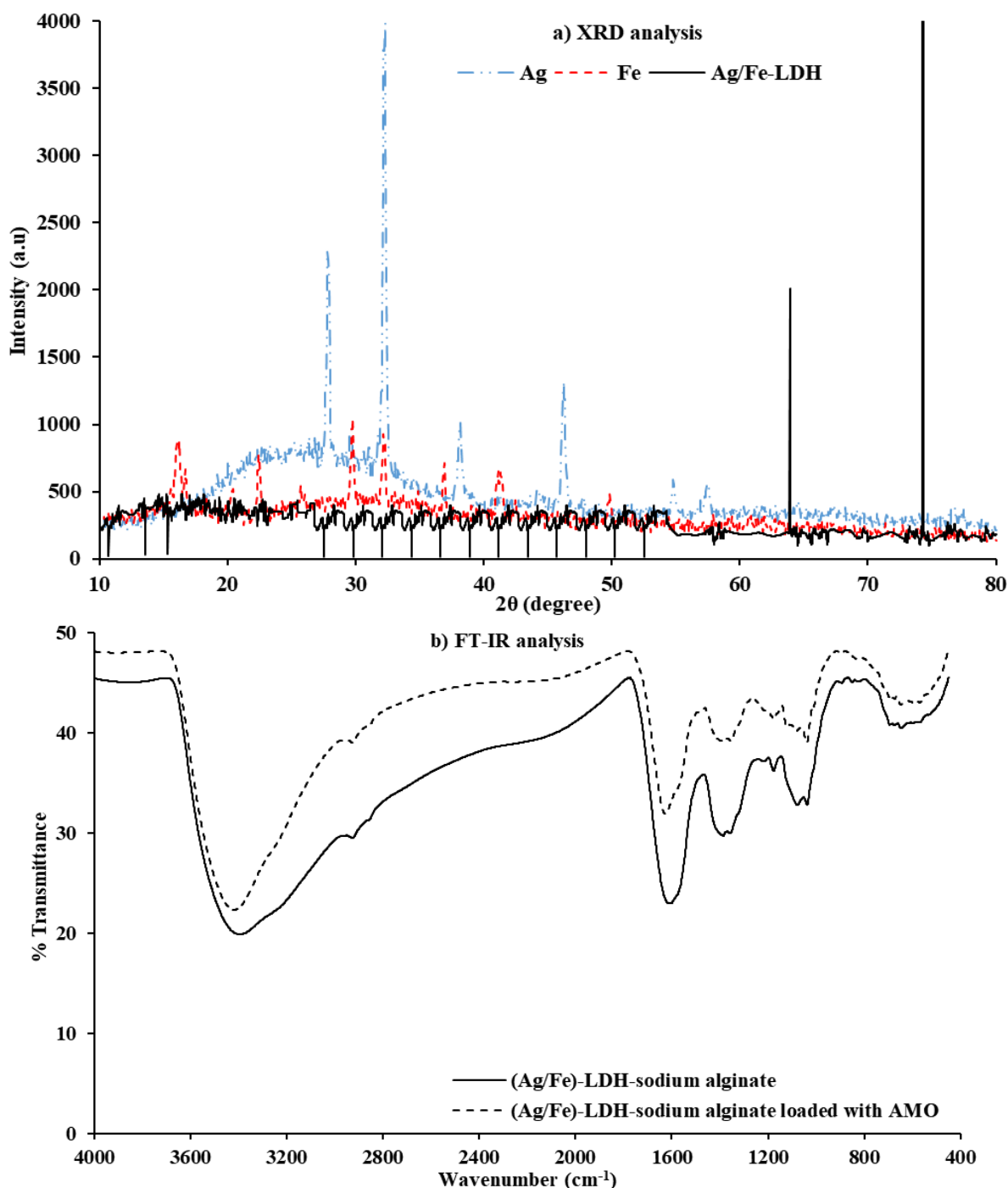

Figure 4. Characterization of prepared Ag/Fe-LDH alginate beads by a) XRD and b) FT-IR analyses
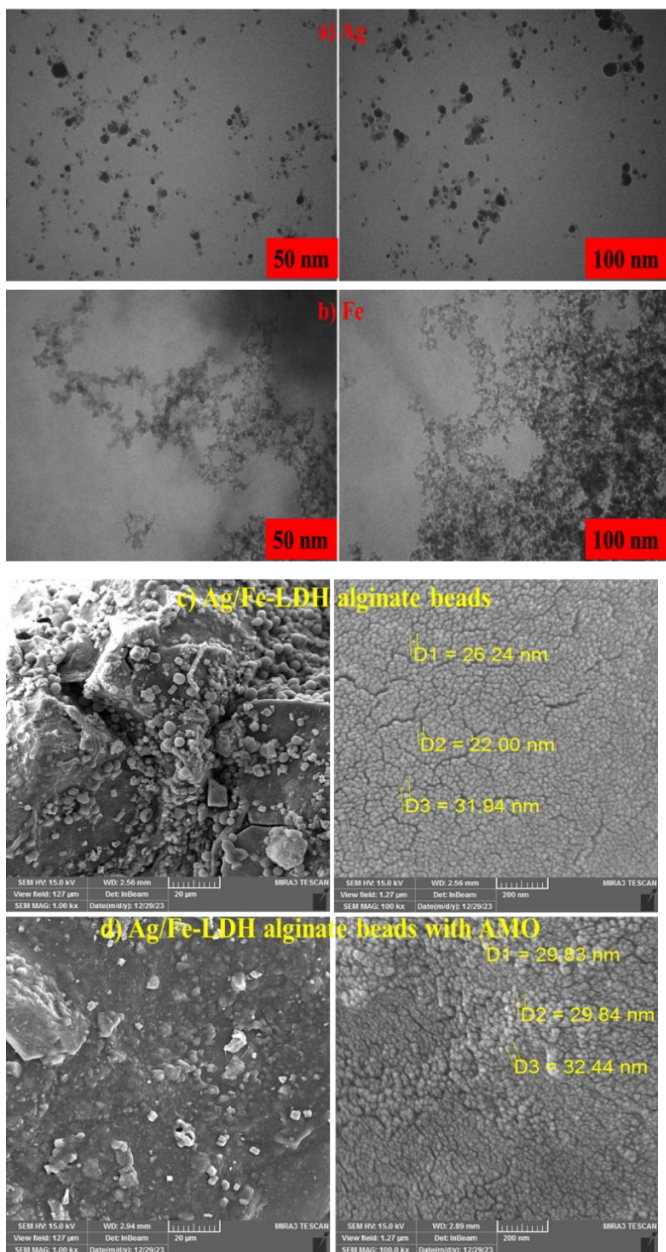
Figure 5. Morphological characteristics using SEM analysis for a) Ag, b) Fe, c) alginate beads, and d) alginate beads loaded with AMO

weak bands of absorption at 1126 and 1026 cm^{-1}, which generated from the -CAO and -CAC- bonds, respectively. A prominent peak is observed at 1053 cm^{-1}, indicating vibrations and stretching of the OH group after the process of AMO sorption. Therefore, the effective elimination of administered antibiotics is achieved through the assistance of the aforementioned groups.

Figure 5(a & b) expressed the morphological characteristics for both Fe and Ag elements. The shape was spherical for both elements. Moreover, the characteristics of prepared beads after and before AMO-interaction can determine by "scanning electron microscopy (SEM)" as plotted in Figure 5(c & d). The pictures demonstrate that the morphology of manufactured sorbent is nonhomogeneous with mean rod particle at 20 µm and 200 nm (Figure 5(c & d)). However, it is worth noting that the beads surfaces are also disordered and highly compact. The beads appear to have a surface with large pores that allow for the oxyanions' sorption. The beads, composed of Ag and Fe, exhibit a fractured surface in comparison to their alginate bead equivalent, indicating a lower level of mechanical strength. Noticeable morphological changes take place in sodium alginate after AMO sorption, as compared to the beads before the sorption.
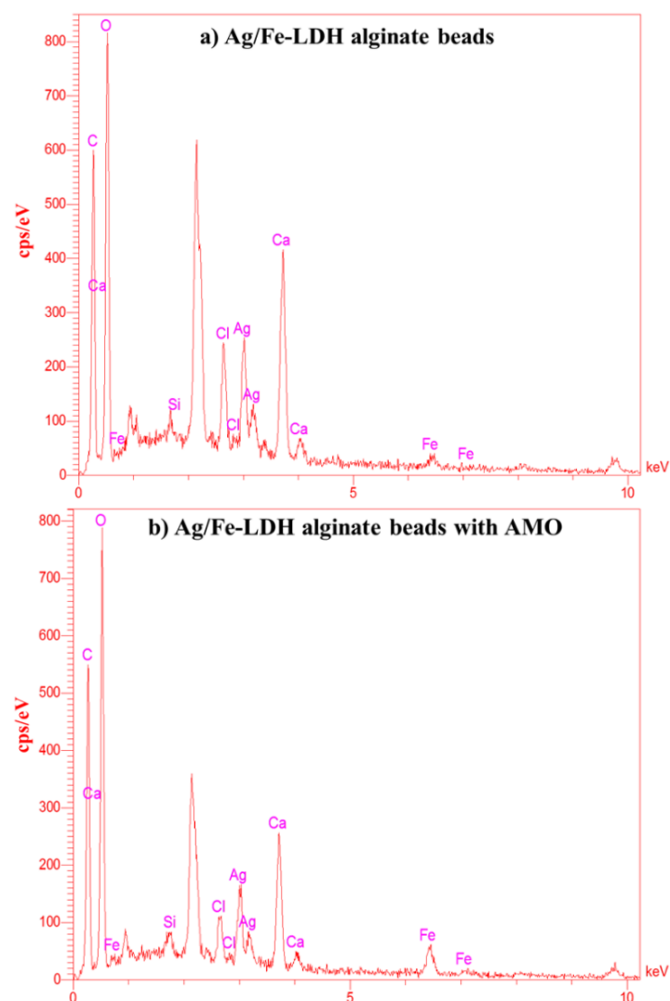
Figure 6. Energy-dispersive spectroscope (EDS) for prepared sorbent

Figure 4(b) presents the infrared absorption spectra for prepared beads after and before AMO sorption. This figure signifies the key functional groups that enhanced AMO sorption. The particles contain –OH (hydroxyl) groups and NAH (amides). The (Ag/Fe)-LDH-sodium alginate exhibited a wide peak, indicating a broad and intense absorption band in the frequency range of 3550-3000 cm^{-1}. This absorption is induced by the stretching mode of OH and NAH groups, and the stretching vibration of hydrogen bonds or the production of interlayer water molecules [32]. The vibrations of the Ag-O lattice and Ag-OH bending are represented by peaks at 893 cm^{-1} [32]. The spectrum explains the existing of characteristic peaks identical to the stretching of CO_2 in the produced alginate, ranging from 1610 to 650 cm^{-1}. The spectrum exhibited two bands of absorption: moderate and weak intensities at frequencies of 1597 and 1411 cm^{-1} respectively. These bands are resulted from the symmetric and asymmetric stretching vibrations of the -COO (carboxylate) group. Additionally, the spectrum illustrated the presence of two

The sorbent's total pore volume and specific surface area are specified by "Brunauer-Emmett-Teller (BET)" analytical method of N2-adsorption/desorption. The silver-iron nanoparticles and prepared beads have surface area of 19.52

and 15.21 m²/g, respectively. The mean pore volume for nanoparticles is 6.333 cm³/g, and 5.518 cm³/g for beads. Furthermore, "Barrett-Joyner-Halenda (BJH)" method is employed to determine the mean pore size of nanoparticles and beads, yielding a value of 0.0178 and 0.0163 nm, respectively. Therefore, the beads have both satisfactory surface area and acceptable overall pore volume. As a result, antibiotic molecules are able to permeate and engage with functional groups, thereby improving their sorption.

The elements percentages in the beads' composition are calculated using EDS graphs as explained in Figure 6. The principal constituents in the prepared sorbent are C, O, Si, Cl, Ca, Fe, and Ag with percentages of 30.84, 45.06, 0.92, 3.17, 9.08, 1.33, and 9.59%, respectively. An increase in the carbon (C) percentage was observed, beyond the sorption of AMO, which confirms the adsorption of antibiotics.

Finally, the color shift is another indication of the stability of silver nanoparticles. A shift in color indicates that silver nanoparticles are aggregating to a bigger size. To verify the function of reducing and capping/stabilizing agents in the synthesis of Ag–Fe bimetallic nanoparticles, "Fourier transform infrared spectroscopy" (FTIR) investigation was carried out. The (EDX) research served as additional confirmation of the successful biosynthesis of Ag–Fe nanoparticles. All these tests indicate the success of the synthesis of the (Ag/Fe)-LDH-sodium alginate.

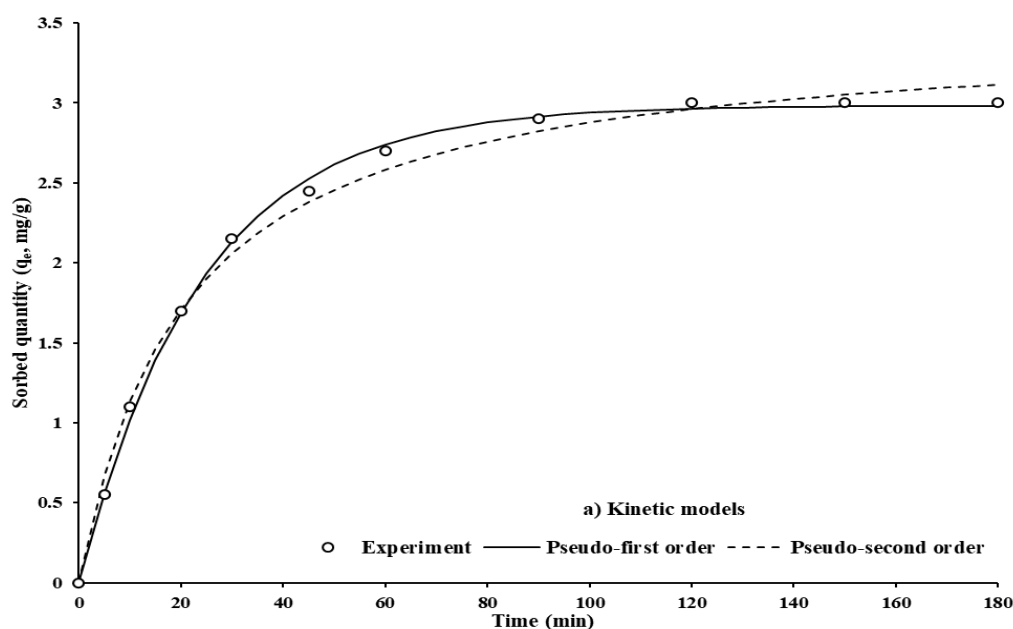## 4.5 Kinetics and isotherm of sorption measurements

The experimental sorption measurements of the AMO over time onto alginate beads were formulated using kinetic models. The formulation procedure requires to fit the sorption data with kinetic models utilizing the "Solver" function in Excel 2016 [33-35]. Table 2 presents the values of parameters for kinetic models. The table confirms that the present models can represent the interaction between AMO and prepared beads. This is evident from Figure 7(a) with the determination coefficient (R^2) and sum of squared error (SSE) inserted in Table 2. Accordingly, the sorption of AMO onto alginate beads is accomplished through physical and chemical forces.

The diffusion model and its constants are also employed through finding the relationship between q_t and t as illustrated

Table 2 and Figure 7(b). This figure illustrates that the relationship can represent by straight lines having intercept with y-axis. Therefore, it may be inferred that the process of AMO sorption necessitates intra-particle diffusion, albeit the specific step that controls the rate of the process is not indicated. This curve exhibits multi-linearity, indicating the simultaneous involvement of two or more mechanisms in the sorption of AMO. The lines in "portion 1" have a steep slope, indicating a high removal rate of contaminants during the early sorption phase [36, 37] and this occurs by external surface sorption. The line of "portion 2" has gradually changes in the slope; so, intra-particle diffusion is governed the rate. Ultimately, "portion 3" signifies the phase of balance that can be associated with the deceleration of diffusion caused by a diminished concentration of contaminants left in the liquid [33-35].

Table 2. Constants of isotherm and kinetic models with statistical measures for sorption of amoxicillin onto Ag/Fe-LDH- alginate beads

Model	Parameter	Value
Freundlich	K_f (mg/g) (L/mg)$^{1/n}$	0.372
	n	1.511
	R^2	0.874
Langmuir	q_{max} (mg/g)	9.512
	b (L/mg)	0.020
	R^2	0.853
Pseudo-first order	q_e (mg/g)	2.984
	k_1 (1/min)	0.042
	R^2, SSE	0.999, 0.17
Pseudo-second order	q_e (mg/g)	3.471
	k_2 (g/mg min)	0.014
	R^2, SSE	0.999, 0.068
Intra-particle diffusion	Portion 1	
	k_{int} (mg/g min$^{0.5}$), C	0.488, 0.498
	R^2	0.996
	Portion 2	
	k_{int} (mg/g min$^{0.5}$), C	0.188, 1.171
	R^2	0.965
	Portion 3	
	k_{int} (mg/g min$^{0.5}$), C	0.024, 2.701
	R^2	0.647

a) Kinetic models

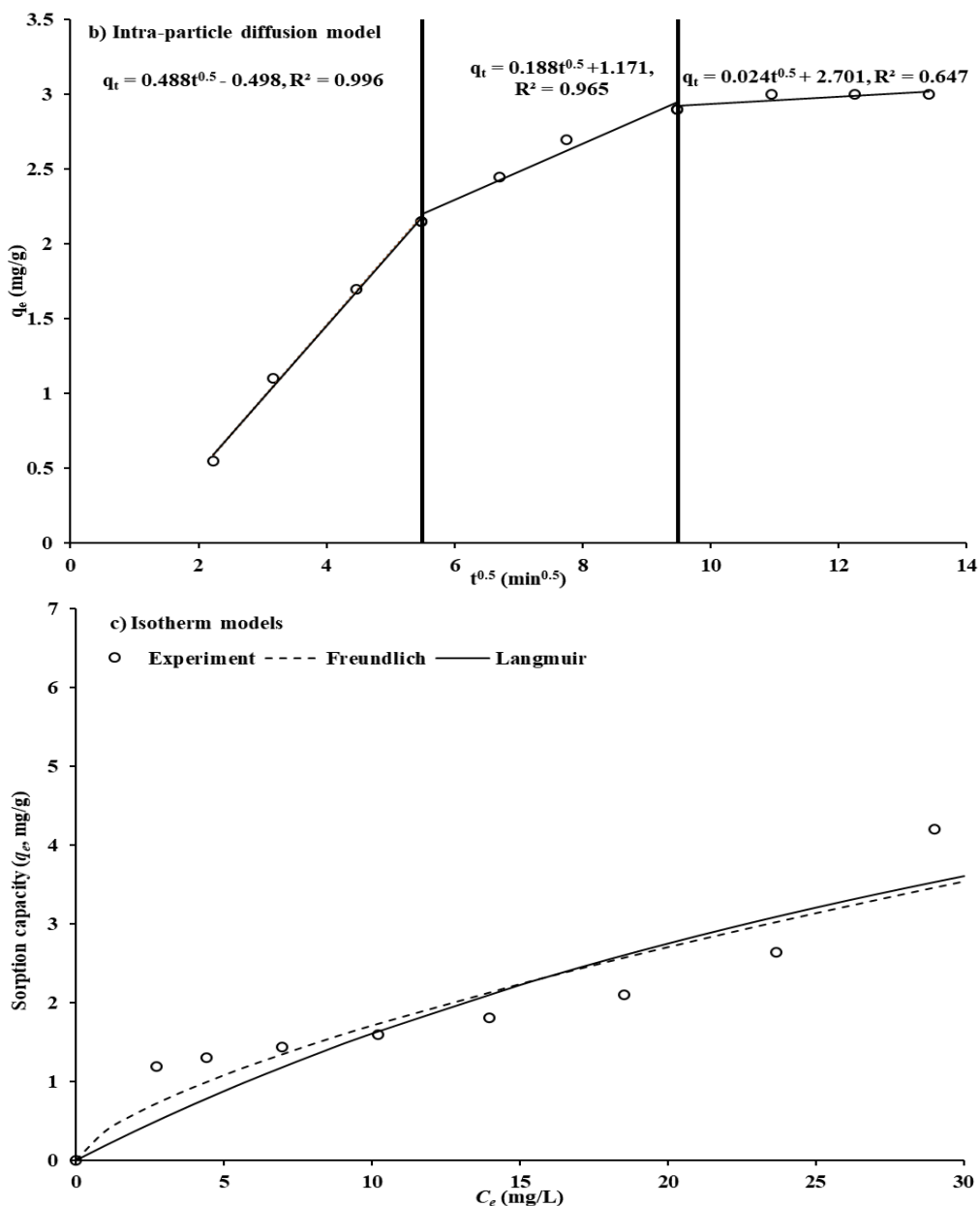○ Experiment —— Pseudo-first order - - - - Pseudo-second order

Figure 7. Formulation of sorption measurements using a) kinetic models, b) intra-particle diffusion model, and c) isotherm models for interaction of Ag/Fe-LDH beads with water contained AMO

Equilibrium isotherms are selected to accurately depict the experimental results of the sorption process once it reached equilibrium. It was crucial to determine the suitable isotherm model by using well-known statistical metrics such as R^2 and SSE. This was necessary in order to calculate the sorption term in the equation used to represent the movement of contaminants in the groundwater [38]. The values of parameters for equilibrium models (Table 2) are determined using "Solver" feature in Excel program 2016. The Langmuir and Freundlich models demonstrate a strong capability in accurately representing the AMO sorption on the produced beads, as evidenced by the high values of R^2 [39]. The concurrence of the experimental results with outcomes of sorption models is signified in Figure 7(c). This agreement can also be recognized by the high coefficient of determination. The AMO sorption capacity reaches a maximum value of 9.512 mg/g, indicating that the sorbent has high capability for AMO elimination [40]. The Freundlich constant (K_F) for AMO adsorption onto alginate beads was determined to be 0.372 (mg/g) (L/mg)$^{1/n}$, where (n) > 1. Therefore, the isotherm

curves can be classified as "favorable" [41, 42]. Table 3 lists a comparison between the q_{max} of AMO onto the present beads and other materials studied previously. The q_{max} of beads appears to be similar to the sorption capacities of sorbents mentioned in the previous studies [43, 44].

Adsorption process is performed in this study for wastewater treatment [53, 54]. Ali et al. [55] employed environmentally friendly methods of biosynthesis to create V_2O_5NPs nanoparticles from vanadium sulfate (VSO$_4$) with minimal effort and expense. Combine 0.1M of Punica Granatum aqueous extract with a basic media ranging from 8 to 12 pH to produce H_2O. The results were compared to those of the gold standard medicine, Amoxicillin. At a concentration of 75%, nano-oxide was determined to be more effective.

Similar studies have performed by Ali and AL-Mammar [56], a low cost, low environmental impact, and lack of toxicity, green synthesis methods have become popular for synthesizing nano-oxides. The aqueous extract of Laurus nobilis leaves was used as a natural capping agent in this study to produce nickel oxide nanoparticles (NiO-NPs). Using an

adsorption approach, the produced NiO-NPs were used to remove Biebrich Scarlet (BS) color from an aqueous solution. According to the kinetic analysis, the adsorption process was better represented by the Pseudo-second-order (PSO) model than by the Pseudo-first-order (PFO) model [53].

Table 3. Maximum adsorption capacities of Ag/Fe-LDH-alginate beads compared with other adsorbents in previous studies for amoxicillin

Sorbent	q_{max} (mg/g)	pH	Time	C_o (mg/L)	Ref.
ATMa clay	9.68	3	24 h	100	[45]
Nano-magnetic walnut shell-rice husk	7.283	6	250 min	100	[37]
A-Fe$_2$O$_3$/RGO	9.69	7	40 min	10	[36]
Cu-immobilized alginate beads	53.25	3	1440min	90	[6]
MnFe$_2$O$_4$/rGO	41	3.3	900 min	10	[46]
GO/Fe$_3$O$_4$-SrTiO$_3$	65.78	4	180 min	100	[47]
Hydroxyapatite/ pumice	17.87	9	180 min	100	[48]
Activated carbon nanoparticles of vine wood	1.98	2	8 h	20	[49]
Graphene oxide-magnetic particles	18.3	3-10	10 min	50	[50]
Granular sludge	15.22	----	36 h	20	[51]
Kaolinite	4.32	7	24 h	----	[52]
Ag/Fe-LDH nanoparticles	9.512	7	90 min	50	Present work

Finally, adsorption Kinetics explains solute adsorption and adsorbate residence time on the solid-liquid interface. Adsorption isotherms determine the optimum adsorbent capacity and adsorbate-adsorbent interaction. Adsorption kinetics is used to evaluate reaction limiting stage, mechanism, and entire adsorption process. Various kinetic models for adsorption research were performed for Ag/Fe-LDH beads. Adsorption experimental data are examined for better fitting in kinetic models, like isotherms. The results reveals that the diffusion kinetic model best explains AMO removal sorption kinetics.

5. CONCLUSIONS

The Ag and Fe ions were successfully extracted from pomegranate peels and sesban tree leaves, which were produced in large quantities as solid waste. In order to create (Ag/Fe)-LDH nanoparticles using the precipitation method, the ions must be mixed together. The use of such wastes considers the actual step in the application of sustainable ideas. In order to create spherical beads, the produced nanoparticles were immobilized with sodium alginate. Batch experiments were used to assess the spherical beads' ability to extract AMO from aqueous solution. Nanoparticle dosage of 7 grams per 100 mL, pH 9 and a molar ratio of (Ag/Fe) = 0.5 were the ideal conditions for the production of beads. Results implied that the appropriate conditions expected to guarantee the expulsion proficiency of AMO> 90% are time 90 min, pH 7, and dose 2 grams per 50 mL for C_o 50 mg/L at 250 rpm. Model of

Langmuir is able to depict the sorption interaction with high capacity of 9.512 mg/g. Results proved that there are physical and chemical forces correlated between molecules of AMO and beads because of the applicability of Pseudo 1st and 2nd order models. The formation of silver/iron-LDH nanoparticles in the prepared beads is certified through characterization analyses; yet, the rise in the carbon percentages indicates the presence of AMO sorption.

All in all, antibiotics and other organic pollutants are among the most worrisome substances for the environment on a worldwide scale. Consequently, a number of eco-friendly, cost-effective, and efficient approaches have been researched and developed over the years to enable the successful removal of these contaminants. the (Ag/Fe)-LDH nanoparticles have many desirable qualities that make them an excellent choice for environmental remediation projects, including being non-toxic, biocompatible, economical, having a natural origin, being easy to use, and being very effective at removing various contaminants.

REFERENCES

[1] Joseph, J., Iftekhar, S., Srivastava, V., Fallah, Z., Zare, E.N., Sillanpää, M. (2021). Iron-based metal-organic framework: Synthesis, structure and current technologies for water reclamation with deep insight into framework integrity. Chemosphere, 284: 131171. https://doi.org/10.1016/j.chemosphere.2021.131171

[2] Alshehri, S.M., Naushad, M., Ahamad, T., Alothman, Z.A., Aldalbahi, A. (2014). Synthesis, characterization of curcumin based ecofriendly antimicrobial bio-adsorbent for the removal of phenol from aqueous medium. Chemical Engineering Journal, 254: 181-189. https://doi.org/10.1016/j.cej.2014.05.100

[3] Karimi-Maleh, H., Khataee, A., Karimi, F., Baghayeri, M., Fu, L., Rouhi, J., Karaman, J., Karaman, O., Boukherroub, R. (2022). A green and sensitive guanine-based DNA biosensor for idarubicin anticancer monitoring in biological samples: A simple and fast strategy for control of health quality in chemotherapy procedure confirmed by docking investigation. Chemosphere, 291: 132928. https://doi.org/10.1016/j.chemosphere.2021.132928

[4] Qiu, M., Liu, L., Ling, Q., Cai, Y., Yu, S., Wang, S.,Fu, D., Hu, B., Wang, X. (2022). Biochar for the removal of contaminants from soil and water: A review. Biochar, 4(1): 19. https://doi.org/10.1007/s42773-022-00146-1

[5] Yang, Y., Ok, Y.S., Kim, K.H., Kwon, E.E., Tsang, Y.F. (2017). Occurrences and removal of pharmaceuticals and personal care products (PPCPs) in drinking water and water/sewage treatment plants: A review. Science of the Total Environment, 596: 303-320. https://doi.org/10.1016/j.scitotenv.2017.04.102

[6] Zhang, X., Lin, X., He, Y., Chen, Y., Luo, X., Shang, R. (2019). Study on adsorption of tetracycline by Cu-immobilized alginate adsorbent from water environment. International journal of biological macromolecules, 124: 418-428. https://doi.org/10.1016/j.ijbiomac.2018.11.218

[7] Ahmed, D.N., Naji, L.A., Faisal, A.A., Al-Ansari, N., Naushad, M. (2020). Waste foundry sand/MgFe-layered double hydroxides composite material for efficient removal of Congo red dye from aqueous solution. Scientific Reports, 10(1): 2042.

https://doi.org/10.1038/s41598-020-58866-y

[8] Faisal, A.A., Ahmed, M.D. (2014). Remediation of groundwater contaminated with copper ions by waste foundry sand permeable barrier. Journal of Engineering, 20(9): 62-77.

[9] Faisal, A.A.H., Nassir, Z.S. (2016). Modeling the removal of cadmium ions from aqueous solutions onto olive pips using neural network technique. Al-Khwarizmi Engineering Journal, 12(3): 1-9.

[10] Li, H.Q., Hu, J.H., Wang, C., Wang, X.J. (2017). Removal of amoxicillin in aqueous solution by a novel chicken feather carbon: Kinetic and equilibrium studies. Water, Air, & Soil Pollution, 228: 201. https://doi.org/10.1007/s11270-017-3385-6

[11] Rashid, H.M., Faisal, A.A.H. (2018). Removal of dissolved cadmium ions from contaminated wastewater using raw scrap zero-valent iron and zero valent aluminum as locally available and inexpensive sorbent wastes. Iraqi Journal of Chemical and Petroleum Engineering, 19(4): 39-45. https://doi.org/10.31699/IJCPE.2018.4.5

[12] Rashid, H.M., Faisal, A.A.H. (2019). Removal of dissolved trivalent chromium ions from contaminated wastewater using locally available raw scrap iron-aluminum waste. Al-Khwarizmi Engineering Journal, 15(1): 134-143. https://doi.org/10.22153/kej.2019.03.006

[13] Wang, Y., Gong, S., Li, Y., Li, Z., Fu, J. (2020). Adsorptive removal of tetracycline by sustainable ceramsite substrate from bentonite/red mud/pine sawdust. Scientific Reports, 10(1): 2960. https://doi.org/10.1038/s41598-020-59850-2

[14] Faisal, A.A., Ahmed, D.N., Rezakazemi, M., Sivarajasekar, N., Sharma, G. (2021). Cost-effective composite prepared from sewage sludge waste and cement kiln dust as permeable reactive barrier to remediate simulated groundwater polluted with tetracycline. Journal of Environmental Chemical Engineering, 9(3): 105194. https://doi.org/10.1016/j.jece.2021.105194

[15] Climent, M.J., Corma, A., Iborra, S., Epping, K., Velty, A. (2004). Increasing the basicity and catalytic activity of hydrotalcites by different synthesis procedures. Journal of Catalysis, 225(2): 316-326. https://doi.org/10.1016/j.jcat.2004.04.027

[16] Mitchell, S., Biswick, T., Jones, W., Williams, G., O'Hare, D. (2007). A synchrotron radiation study of the hydrothermal synthesis of layered double hydroxides from MgO and Al_2O_3 slurries. Green Chemistry, 9(4): 373-378.

[17] Mallkpour, S., Dinari, M., Behranvand, V. (2013). Ultrasonic-assisted synthesis and characterization of layered double hydroxides intercalated with bioactive N, N′-(pyromellitoyl)-bis-l-α-amino acids. RSC Advances, 3(45): 23303-23308. https://doi.org/10.1039/C3RA43645D

[18] Greenwell, H.C., Jones, W., Rugen-Hankey, S.L., Holliman, P.J., Thompson, R.L. (2010). Efficient synthesis of ordered organo-layered double hydroxides. Green Chemistry, 12(4): 688-695.

[19] Shao, M., Han, J., Wei, M., Evans, D.G., Duan, X. (2011). The synthesis of hierarchical Zn–Ti layered double hydroxide for efficient visible-light photocatalysis. Chemical Engineering Journal, 168(2): 519-524.

https://doi.org/10.1016/j.cej.2011.01.016

[20] Wang, C., Jian, J.J. (2015). Degradation and detoxity of tetracycline by an enhanced sonolysis. Journal of Water and Technology, 13(4): 325-334. https://doi.org/10.2965/jwet.2015.325

[21] Abraha, A., Kebede, A., Belay, A. (2016). Study of the self-association of amoxicillin, thiamine and the hetero-association with biologically active compound chlorgenic acid. African Journal of Pharmacy and Pharmacology, 10(18): 393-402. https://doi.org/10.5897/AJPP2016.4542

[22] Arıca, M.Y., Kacar, Y., Genç, Ö. (2001). Entrapment of white-rot fungus Trametes versicolor in Ca-alginate beads: Preparation and biosorption kinetic analysis for cadmium removal from an aqueous solution. Bioresource Technology, 80(2): 121-129. https://doi.org/10.1016/S0960-8524(01)00084-0

[23] Perry, R.H., Chilton, C.H. (1984). Chemical Engineering Handbook. The McGraw-Hill Companies.

[24] Ho, Y.S., Porter, J.F., McKay, G. (2002). Equilibrium isotherm studies for the sorption of divalent metal ions onto peat: Copper, nickel and lead single component systems. Water, Air, and Soil Pollution, 141: 1-33.

[25] Milagres, J.L., Bellato, C.R., Vieira, R.S., Ferreira, S.O., Reis, C. (2017). Preparation and evaluation of the Ca-Al layered double hydroxide for removal of copper (II), nickel (II), zinc (II), chromium (VI) and phosphate from aqueous solutions. Journal of Environmental Chemical Engineering, 5(6): 5469-5480. https://doi.org/10.1016/j.jece.2017.10.013

[26] Faisal, A.A., Naji, L.A. (2019). Simulation of ammonia nitrogen removal from simulated wastewater by sorption onto waste foundry sand using artificial neural network. Association of Arab Universities Journal of Engineering Sciences, 26(1): 28-34. https://doi.org/10.33261/jaaru.2019.26.1.004

[27] Abd Ali, Z.T., Naji, L.A., Almuktar, S.A., Faisal, A.A., Abed, S.N., Scholz, M., Naushad, M., Ahamad, T. (2020). Predominant mechanisms for the removal of nickel metal ion from aqueous solution using cement kiln dust. Journal of Water Process Engineering, 33: 101033. https://doi.org/10.1016/j.jwpe.2019.101033

[28] Wawrzkiewicz, M., Hubicki, Z. (2009). Removal of tartrazine from aqueous solutions by strongly basic polystyrene anion exchange resins. Journal of Hazardous Materials, 164(2-3): 502-509. https://doi.org/10.1016/j.jhazmat.2008.08.021

[29] Prestopino, G., Arrabito, G. (2021). Layered Double Hydroxides. Crystals, MDPI. https://doi.org/10.3390/books978-3-0365-0307-3

[30] Ruan, X., Sun, P., Ouyang, X., Qian, G. (2011). Characteristics and mechanisms of sorption of organic contaminants onto sodium dodecyl sulfate modified Ca-Al layered double hydroxides. Chinese Science Bulletin, 56: 3431-3436. https://doi.org/10.1007/s11434-011-4762-y

[31] Szabados, M., Varga, G., Kónya, Z., Kukovecz, Á., Carlson, S., Sipos, P., Pálinkó, I. (2018). Ultrasonically-enhanced preparation, characterization of CaFe-layered double hydroxides with various interlayer halide, azide and oxo anions (CO_3^{2-}, NO_3^-, ClO_4^-). Ultrasonics Sonochemistry, 40: 853-860. https://doi.org/10.1016/j.ultsonch.2017.08.041

[32] Chen, H., Chen, Z., Zhao, G., Zhang, Z., Xu, C., Liu, Y.,

Chrn, J., Zhuang, L., Haya, T., Wang, X. (2018). Enhanced adsorption of U (VI) and [241]Am (III) from wastewater using Ca/Al layered double hydroxide@ carbon nanotube composites. Journal of Hazardous Materials, 347: 67-77. https://doi.org/10.1016/j.jhazmat.2017.12.062

[33] Cheung, W.H., Szeto, Y.S., McKay, G. (2007). Intraparticle diffusion processes during acid dye adsorption onto chitosan. Bioresource Technology, 98(15): 2897-2904. https://doi.org/10.1016/j.biortech.2006.09.045

[34] Özer, A., Gürbüz, G., Çalimli, A., Körbahti, B.K. (2009). Biosorption of copper (II) ions on Enteromorpha prolifera: Application of response surface methodology (RSM). Chemical Engineering Journal, 146(3): 377-387. https://doi.org/10.1016/j.cej.2008.06.041

[35] Wang, L., Zhang, J., Zhao, R., Li, Y., Li, C., Zhang, C. (2010). Adsorption of Pb (II) on activated carbon prepared from *Polygonum orientale* Linn.: Kinetics, isotherms, pH, and ionic strength studies. Bioresource Technology, 101(15): 5808-5814. https://doi.org/10.1016/j.biortech.2010.02.099

[36] Huízar-Félix, A.M., Aguilar-Flores, C., Martínez-de-la Cruz, A., Barandiarán, J.M., Sepúlveda-Guzmán, S., Cruz-Silva, R. (2019). Removal of tetracycline pollutants by adsorption and magnetic separation using reduced graphene oxide decorated with α-Fe_2O_3 nanoparticles. Nanomaterials, 9(3): 313. https://doi.org/10.3390/nano9030313

[37] Popoola, L.T. (2020). Tetracycline and sulfamethoxazole adsorption onto nanomagnetic walnut shell-rice husk: Isotherm, kinetic, mechanistic and thermodynamic studies. International Journal of Environmental Analytical Chemistry, 100(9): 1021-1043. https://doi.org/10.1080/03067319.2019.1646739

[38] Rajeshkumar, S., Bharath, L.V. (2017). Mechanism of plant-mediated synthesis of silver nanoparticles – A review on biomolecules involved, characterisation and antibacterial activity. Chemico-Biological Interactions, 273: 219-227. https://doi.org/10.1016/j.cbi.2017.06.019

[39] Azarbani, F., Shiravand, S. (2020). Green synthesis of silver nanoparticles by Ferulago macrocarpa flowers extract and their antibacterial, antifungal and toxic effects. Green Chemistry Letters and Reviews, 13(1): 41-49. https://doi.org/10.1080/17518253.2020.1726504

[40] McClelland, J.J., Hill, S.B., Pichler, M., Celotta, R.J. (2004). Nanotechnology with atom optics. Science and Technology of Advanced Materials, 5(5-6): 575-580. https://doi.org/10.1016/j.stam.2004.02.023

[41] Sifonte, E.P., Castro-Smirnov, F.A., Jimenez, A.A.S., Diez, H.R.G., Martínez, F.G. (2021). Quantum mechanics descriptors in a nano-QSAR model to predict metal oxide nanoparticles toxicity in human keratinous cells. Journal of Nanoparticle Research, 23: 1-16. https://doi.org/10.1007/s11051-021-05288-0

[42] Sinha, A., Behera, A. (2022). Nanotechnology in the space industry. In: Nanotechnology-Based Smart Remote Sensing Networks for Disaster Prevention, pp. 139-157. https://doi.org/10.1016/B978-0-323-91166-5.00005-7

[43] Serrano, E., Rus, G., Garcia-Martinez, J. (2009). Nanotechnology for sustainable energy. Renewable and Sustainable Energy Reviews, 13(9): 2373-2384.

[44] Coskun, S., Ates, E.S., Unalan, H.E. (2013). Optimization of silver nanowire networks for polymer light emitting diode electrodes. Nanotechnology, 24(12): 125202. https://doi.org/10.1088/0957-4484/24/12/125202

[45] Hamoudi, S.A., Hamdi, B., Brendlé, J. (2021). Tetracycline removal from water by adsorption on geomaterial, activated carbon and clay adsorbents. Ecological Chemistry and Engineering S, 28(3): 303-328.

[46] Bao, J., Zhu, Y., Yuan, S., Wang, F., Tang, H., Bao, Z., Zhou, H., Chen, Y. (2018). Adsorption of tetracycline with reduced graphene oxide decorated with $MnFe_2O_4$ nanoparticles. Nanoscale Research Letters, 13: 1-8. https://doi.org/10.1186/s11671-018-2814-9

[47] Nodeh, H.R., Sereshti, H. (2016). Synthesis of magnetic graphene oxide doped with strontium titanium trioxide nanoparticles as a nanocomposite for the removal of antibiotics from aqueous media. RSC Advances, 6(92): 89953-89965. https://doi.org/10.1039/C6RA18341G

[48] Ersan, M., Guler, U.A., Acıkel, U., Sarioglu, M. (2015). Synthesis of hydroxyapatite/clay and hydroxyapatite/pumice composites for tetracycline removal from aqueous solutions. Process Safety and Environmental Protection, 96: 22-32. https://doi.org/10.1016/j.psep.2015.04.001

[49] Pouretedal, H.R., Sadegh, N. (2014). Effective removal of amoxicillin, cephalexin, tetracycline and penicillin G from aqueous solutions using activated carbon nanoparticles prepared from vine wood. Journal of Water Process Engineering, 1: 64-73. https://doi.org/10.1016/j.jwpe.2014.03.006

[50] Lin, Y., Xu, S., Li, J. (2013). Fast and highly efficient tetracyclines removal from environmental waters by graphene oxide functionalized magnetic particles. Chemical Engineering Journal, 225: 679-685. https://doi.org/10.1016/j.cej.2013.03.104

[51] Shi, Y.J., Wang, X.H., Qi, Z., Diao, M.H., Gao, M.M., Xing, S.F., Wang, S.G., Zhao, X.C. (2011). Sorption and biodegradation of tetracycline by nitrifying granules and the toxicity of tetracycline on granules. Journal of Hazardous Materials, 191(1-3): 103-109. https://doi.org/10.1016/j.jhazmat.2011.04.048

[52] Li, Z., Schulz, L., Ackley, C., Fenske, N. (2010). Adsorption of tetracycline on kaolinite with pH-dependent surface charges. Journal of Colloid and Interface Science, 351(1): 254-260. https://doi.org/10.1016/j.jcis.2010.07.034

[53] Mohamed, S., Kareem, N. (2018). Optical properties for prepared polyvinyl alcohol/polyaniline/ZnO nanocomposites. Iraqi Journal of Physics, 16(36): 181-189. https://doi.org/10.30723/ijp.v16i36.42

[54] Mousa, S.A., Tareq, S., Muhammed, E.A. (2021). Studying the photodegradation of congo red dye from aqueous solutions using bimetallic Au–Pd/TiO_2 photocatalyst. Baghdad Science Journal, 18(4): 1261-1268. https://doi.org/10.21123/bsj.2021.18.4.1261

[55] Ali, A.T., Karem, L.K.A. (2024). Biosynthesis, characterization, adsorption and antimicrobial studies of vanadium oxide nanoparticles using punica granatum extract. Baghdad Science Journal, 21(2): 410-421. https://doi.org/10.21123/bsj.2023.8114

[56] Ali, O.S., AL-Mammar, D.E. (2024). Adsorption of the color pollutant onto nio nanoparticles prepared by a new green method. Iraqi Journal of Science, 65(4): 1824-1838. https://doi.org/10.24996/ijs.2024.65.4.4